25th IUPAP Conference on Computational Physics (CCP2013) IOP Publishing
Journal of Physics: Conference Series **510** (2014) 012034 doi:10.1088/1742-6596/510/1/012034

Dynamics of Two-dimensional Electron Gas in Non-uniform magnetic field

O G Balev[1] and I A Larkin[2,3]

Abstract.
We have theoretically studied dynamics of the two-dimensional electron system (2DES) placed in a strong laterally non-uniform magnetic field, which appears due to ferromagnetic film on the top of heterostructure. It is shown that lateral inhomogeneity of a strong magnetic field allows itself "magnetic gradient" or special magnetic-edge magnetoplasmons. This mechanism is different from usual "density gradient" edge magnetoplasmons. We have solved self-consistently Poisson equation for non-uniform density distribution of the 2DES for realistic heterostructure together with hydrodynamic equation of 2D Fermi liquid. As a result eigen value problem has been obtained that corresponds to the motion of charge density wave perpendicular to magnetic gradient. It is shown that for non-monotonic distribution of magnetic field "magnetic gradient" magnetoplasmons may move in both directions. To solve eigen value problem we have compared two types of numerical approaches: first is grid method that diagonalizes large Hermitian matrix and second is semi-analytical approach that expand each eigen mode on the set of orthogonal functions.

[1] Departamento de Física, Universidade Federal do Amazonas, 69077-000, Manaus, AM, Brazil
[2] Department of Physics, Minho University, Braga 4710-057, Portugal
[3] Institute of Microelectronics Technology RAS, 142432 Chernogolovka, Russia

E-mail: ogbalev@ufam.edu.br
vaniala2000@yahoo.co.uk

Edge magnetoplasmons (EMPs) have been studied for 2DES subjected to a lateral confining potential and a strong homogeneos magnetic fiels [1, 2, 3, 4, 5]. The EMPs appear due to a strong change of the stationary local electron density at the edge of the channel that induces a strong modulation of the local magnetoconductivity [1, 3, 5] and can be charactarized also as "density gradient" EMPs [6]. Recently [6] the chiral modes in 2DES induced by the lateral inhomogeneity of a strong magnetic field and named magnetic-edge magnetoplasmons (MEMPs), or "magnetic gradient" edge magnetoplasmons, have been studied. They are localized in a vicinity of magnetic-edge, i.e., the region of magnetic field inhomogeneity. Here we present new results on MEMPs. In particular, for conditions when modulation of the magnetic field, within 2DES, is not very small in comparison with a finite external spatially homogeneous magnetic field; here purely symmetric or antisimmetric MEMPs will be absent.

We consider homogeneous 2DES, localized within $z = 0$ plane, that is embedded in GaAs based sample, with the dielectric constant ε, that occupies a half-space $z < d$. In addition, 2DES is subjected to a strong laterally inhomogeneos magnetic field $\mathbf{B}(y) = B(y)\hat{\mathbf{z}}$, which appears due to ferromagnetic semi-infinite film of a finite thickness ηd. This film is located at $y < 0$, $d(1 + \eta) > z > d$. Fig. 1 presents a model geometry under discussion; the x-axis points out of the figure plane. A finite external spatially homogeneous magnetic field $\mathbf{B}_{ext} = B_{ext}\hat{\mathbf{z}}$ is applied as well; $B_{ext} > 0$. We assume that the surface of heterostructure crystal, at $z = d$, has

pined potential [7], or covered by a very thin (of the thichness $\ll d$) homogeneous nonmagnetic-metallic gate. In addition, we assume that at $z = 0$ plane the ions jellium background of the constant area density n_I is located. Following Ref. [6], we assume that magnetic field $B(y)$ is a smooth function of y, with the characteristic scale Δy and the static electron density is well approximated by n_I.

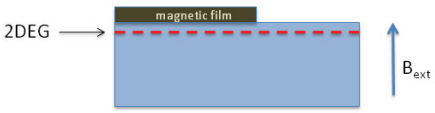

Figure 1. 2DES, at $z = 0$, is embedded in heterostructure, $z < d$. Potential at $z = d$ is pined. Ferromagnetic semi-infinite film ($y < 0$, $d < z < d(1 + \eta)$) induces inhomogeneity of magnetic field within 2DES.

Following [6], for the low-frequency and the long-wavelength conditions, the current density induced by a wave can be calculated in the quasi-static approximation as

$$j_x(y) = \sigma_{xx}(y)E_x(y) - \sigma^0_{yx}(y)E_y(y), \quad j_y(y) = \sigma_{yy}(y)E_y(y) + \sigma^0_{yx}(y)E_x(y), \tag{1}$$

where we have suppressed the exponential factor $\exp[-i(\omega t - k_x x)]$ and common arguments ω, k_x in $j_\mu(y)$, $E_\mu(y)$. Dissipation is neglected, assuming a clean 2DES and sufficiently low temperatures T [6].

For our setup, shown in Fig. 1, we assume that magnetic moment of the ferromagnetic semi-infinite film is constant, $\mathbf{M}_0 = M_0\hat{\mathbf{z}}$. Then readily it follows [8, 6] that

$$B(y) = B_{ext} - 2M_0\{\arctan(Y) - \arctan(Y/(1+\eta))\}, \tag{2}$$

where $Y = y/d$. We assume that $B_0 > 0$ and $M_0/B_{ext} \leq 1$.

Figure 2. Dimensionless phase velocity for six most fast symmetric MEMPs, for $2M_0/B_{ext} \ll 1$, as function of η. MEMPs of both positive and negative chirality are present.

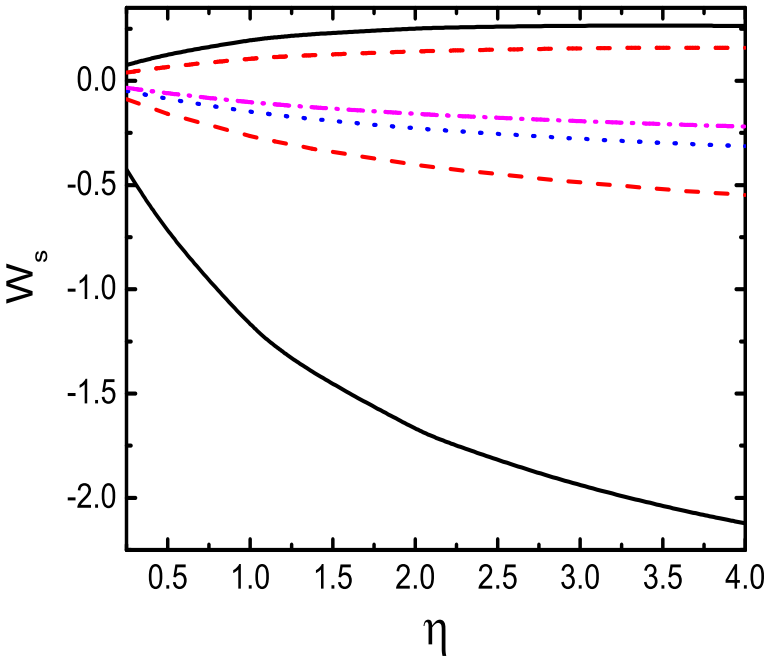

Figure 3. Dimensionless phase velocity for six most fast antisymmetric MEMPs, for $2M_0/B_{ext} \ll 1$, as function of η. MEMPs of both positive and negative chirality are present.

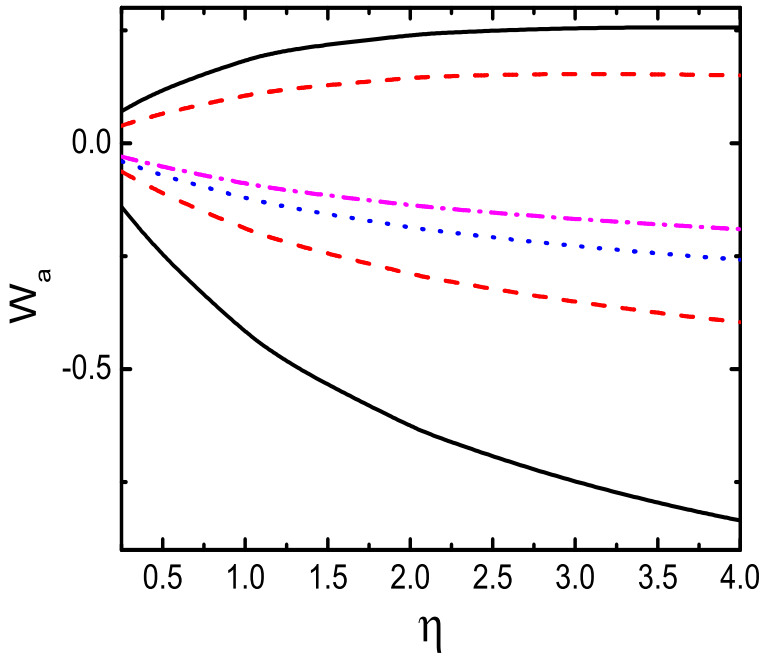

For $B(y)$ given by Eq. (2), using Eq. (1), the Poisson equation and the continuity equation, we obtain the integral equation for the wave charge density $\rho(\omega, k_x, Y)$ as

$$\frac{\omega}{k_x}\rho(\omega,k_x,Y) - \frac{2|e|cn_I}{\varepsilon B_0} g_0(Y) f_0(Y) \int_{-\infty}^{\infty} dY' \rho(\omega,k_x,Y') R_g^{(0)}(|Y-Y'|;k_x d) = 0, \tag{3}$$

where $B_0 = B_{ext}^2/(4M_0)$, exact dimensionless gradient $B(y)$ along y is given by

$$g_0(Y) = \{\frac{(1+\eta)^{-1}}{1+Y^2/(1+\eta)^2} - \frac{1}{1+Y^2}\}. \tag{4}$$

and prefactor

$$f_0(Y) = \{1 - \frac{2M_0}{B_{ext}}[\arctan(Y) - \arctan(\frac{Y}{1+\eta})]\}^{-2}. \tag{5}$$

In $R_g^{(0)}(|Y-Y'|;k_x d)$ we took the screening of the Coulomb potential by the equipotential surface at $z = d$ into account, namely:

$$R_g^{(0)}(|Y-Y'|;k_x d) = K_0(|k_x d||Y-Y'|) - K_0(|k_x d|\sqrt{(Y-Y')^2+4}), \tag{6}$$

where $K_0(x)$ is the modified Bessel function. We assume that $k_x d \ll 1$. Eqs. (3)-(6) show that at $k_x \to 0$ the magnetic edge waves have acoustic type of dispersion.

To solve equation (3) numerically, we use two methods. The first one is a grid approximation, where we use uniform grid with step $\Delta Y = 0.02$ with span $Y \in [-19, 19]$. As a result, equation (3) is approximated by large Hermitian matrix and eigen values of this matrix correspond to eigen values of equation (3). The drawback of this approach is that it is not an accurate approximation of equation (3) at $Y \to \pm\infty$.

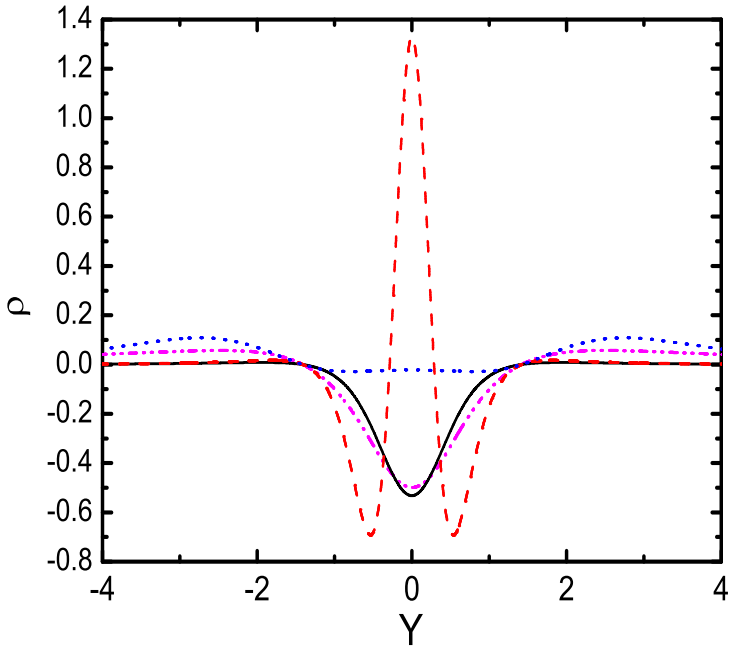

Figure 4. Spatial profiles, at $\eta = 1$, for three fastest symmetric MEMPs are plotted by the solid curve, for $W_s = -1.175255$, the dashed curve, for $W_s = -0.265200$, and the dotted curve, for $W_s = 0.196089$. The dot-dot-dashed curve plots $g_0(Y)$.

Another way to solve equation (3) numerically is to introduce a new variable $X = \frac{2}{\pi}\arctan(Y)$ that varies from -1 to 1 while Y changes from $-\infty$ to ∞. In Eq. (4) as function of X the left hand side we will denote as $g_0(X)$, to simplify notations. First, we consider the limit $M_0/B_{ext} \ll 1$ where we approximate $1/B(Y)$ as

$$\frac{1}{B(y)} \approx \frac{1}{B_{ext}} - \frac{1}{2B_0}\{\arctan(Y/(1+\eta)) - \arctan(Y)\}, \tag{7}$$

in this approximation prefactor $f_0(Y) = 1$. In Ref. [6] it is shown that Eq. (3) at $f_0(Y) = 1$ has a complete set of solutions can be presented as the set of symmetric solutions and the set of antisymmetric solutions.

Then the symmetric solutions of Eq. (3) are given as [6]

$$\rho_s(\omega, k_x; X) = g_0(X) \sum_{k=0}^{\infty} a_k^s(\omega, k_x) \left[\cos(k\pi X) - \frac{1}{2}\delta_{k,0}\right], \tag{8}$$

and they are defined by the system of linear homogeneous equations

$$W a_n^s - \sum_{k=0}^{\infty} r_{n,k}^s a_k^s = 0, \tag{9}$$

where $n = 0, 1, 2, ...$; $\delta_{k,0}$ is the symbol Kroneckera, the matrix elements

$$r_{n,k}^s = \frac{\pi}{2}\int_{-1}^{1} dX \cos(n\pi X) \int_{-1}^{1} dX' R_g^{(0)}(|\tan(\frac{\pi}{2}X) - \tan(\frac{\pi}{2}X')|, |k_x d|)$$
$$\times \left[\frac{1+\eta}{1+\eta(2+\eta)\cos^2(\pi X'/2)} - 1\right]\left[\cos(k\pi X') - \frac{1}{2}\delta_{k,0}\right], \tag{10}$$

$W = \frac{\omega}{k_x}\frac{\varepsilon B_0}{2|e|cn_I}$ is the dimensionless wave velocity and its sign corresponds to a sign of the chirality or of the phase velocity. On Fig. 2 we plot dimensionless phase velocity W_s as function of η for six most fast symmetric MEMPs calculated from Eq. (9). In Fig. 2 it is seen that $|W_s|$ of the most fast MEMP with the negative chirality is much larger than W_s of the most fast MEMP with the positive chirality.

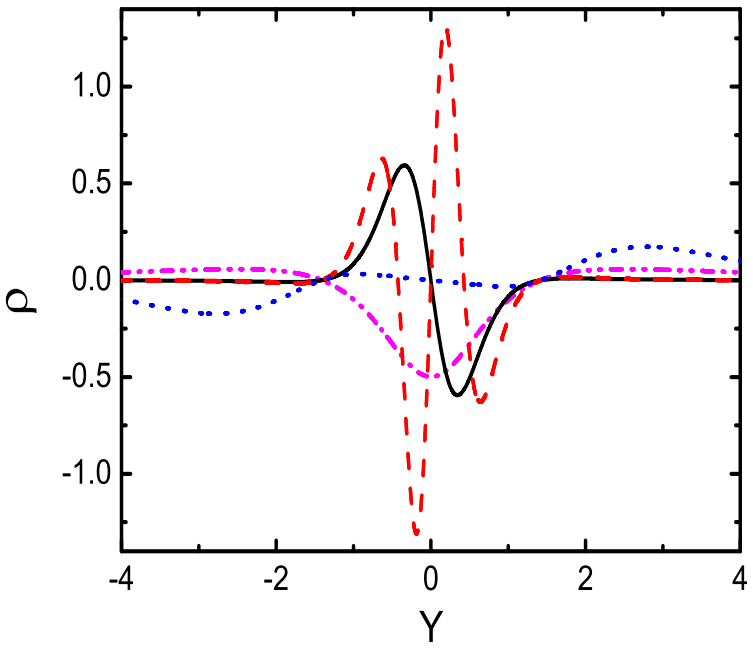

Figure 5. Spatial profiles, at $\eta = 1$, for three fastest antisymmetric MEMPs are plotted: by the solid curve, for $W_s = -0.418959$, the dashed curve, for $W_s = -0.189269$, and the dotted curve, for $W_s = 0.185154$. The dot-dot-dashed curve plots $g_0(Y)$.

The antisymmetric solutions of Eq. (3) are given as

$$\rho_a(\omega, k_x; X) = g_0(X) \sum_{k=1}^{\infty} a_k^a(\omega, k_x) \sin(k\pi X), \tag{11}$$

and they are defined by the system of linear homogeneous equations

$$W a_n^a - \sum_{k=1}^{\infty} r_{n,k}^a a_k^a = 0, \tag{12}$$

where $n = 1, 2, 3, ...$; the matrix elements

$$r_{n,k}^a = \frac{\pi}{2}\int_{-1}^{1} dX \sin(n\pi X) \int_{-1}^{1} dX' R_g^{(0)}(|\tan(\frac{\pi}{2}X) - \tan(\frac{\pi}{2}X')|, |k_x d|)$$
$$\times \left[\frac{1+\eta}{1+\eta(2+\eta)\cos^2(\pi X'/2)} - 1\right] \sin(k\pi X'). \tag{13}$$

Eq. (9) and Eq. (12) have infinite set of positive and negative eigen values, however, physically only a finite number of these modes, with largest $|W|$, meet assumed conditions as slower modes

have the characteristic scale of the spatial structure along y of the order of magnetic length or smaller. On Fig. 3 we plot dimensionless phase velocity W_a as function of η for six most fast antisymmetric MEMPs calculated from Eq. (12). In Fig. 3 it is seen that $|W_a|$ of the most fast MEMP with the negative chirality is essentially larger than W_a of the most fast MEMP with the positive chirality. From Figs. 2, 3 it follows that the fastest mode is the fundamental symmetric MEMP which has negative chirality (as well as the sign of velocity) and only two nodes that coincide with the nodes of $g_0(Y)$. The latter is a common factor for obtained density profiles Eqs. (8), (11).

In Fig. 4, using Eqs. (8)-(9), and Fig. 5, by using Eqs. (11)-(12), we plot charge density profiles of three fastest symmetric and antisymmetric modes for $\eta = 1$; $g_0(Y)$ is also shown. It is seen that for the modes with the negative chirality the wave charge density is strongly localized within the region of negative $g_0(Y)$, i.e, $-1.75 \leq Y \leq 1.75$. In addition, in Figs. 4, 5 the charge density of the MEMPs with the positive chirality, is more localized within the region of positive $g_0(Y)$, at $|Y| > 1.75$.

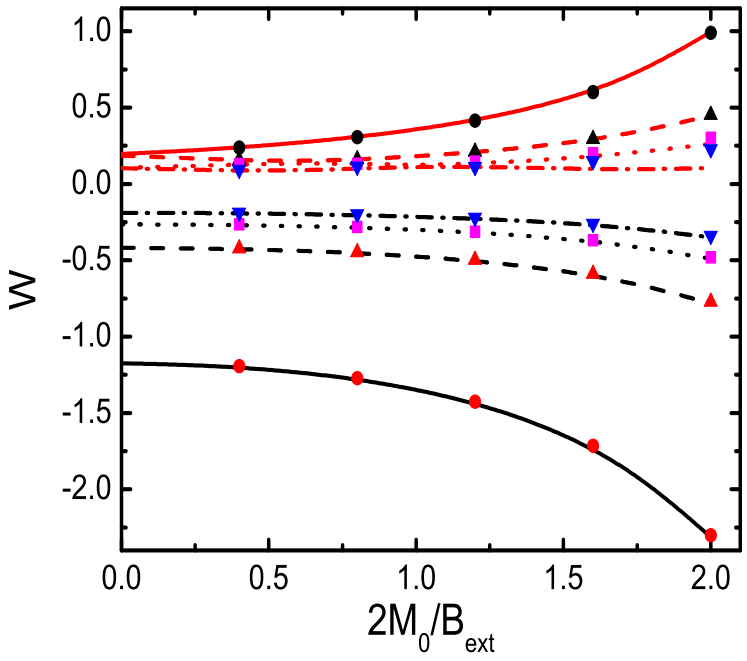

Figure 6. Dimensionless phase velocities for four most fast MEMPs with negative chirality and four most fast MEMPs with positive chirality as function of $2M_0/B_{ext}$, for $\eta = 1$, calculated from Eqs. (17). With full circles, triangles, squares, and upside-down triangles we show results for pertinent MEMPs calculated by another numerical approach, where equation (3) was approximated by the grid with step $\Delta Y = 0.02$ on finite domain [-19,19].

If exact form of $f_0(Y)$ is taken into account, Eq. (3) readily reduces to the integral equation for the wave charge density $\rho(\omega, k_x, X)$ as

$$W\rho(\omega, k_x, X) - g_0(X)f_0(X)\int_{-1}^{1} \frac{(\pi/2)dX'}{\cos^2(\pi X'/2)}\rho(\omega, k_x, X')R_g^{(0)}(|\tan(\frac{\pi}{2}X) - \tan(\frac{\pi}{2}X')|; k_x d) = 0, \tag{14}$$

where factor

$$f_0(X) = \{1 - \frac{2M_0}{B_{ext}}[\frac{\pi}{2}X - \arctan(\frac{1}{1+\eta}\tan(\frac{\pi}{2}X))]\}^{-2}. \tag{15}$$

From Eq. (14) it follows that its solutions are not either symmetric or antisymmetric, so we look for its solutions in the form

$$\rho(\omega,k_x;X)=g_0(X)f_0(X)\{\sum_{k=0}^{\infty}a_k(\omega,k_x)\left[\cos(k\pi X)-\frac{1}{2}\delta_{k,0}\right]+\sum_{l=1}^{\infty}b_l(\omega,k_x)\sin(l\pi X)\}. \quad (16)$$

Then Eq. (14) is reduced to the system of linear homogeneous equations

$$Wa_n-\{\sum_{k_1=0}^{\infty}r^{a,1}_{n,k_1}a_{k_1}+\sum_{k_2=0}^{\infty}r^{b,1}_{n,k_2}b_{k_2}\}=0,\quad Wb_m-\{\sum_{k_3=0}^{\infty}r^{a,2}_{m,k_3}a_{k_3}+\sum_{k_4=0}^{\infty}r^{b,2}_{m,k_4}b_{k_4}\}=0, \quad (17)$$

where $n,k_1,k_3=0,1,2,3,...$ and $m,k_2,k_4=1,2,3,...$; the matrix elements

$$r^{a,1}_{n,k}=\frac{\pi}{2}\int_{-1}^{1}dX\cos(n\pi X)\int_{-1}^{1}dX'R_g^{(0)}(|\tan(\frac{\pi}{2}X)-\tan(\frac{\pi}{2}X')|,|k_xd|)$$
$$\times f_0(X')\left[\frac{1+\eta}{1+\eta(2+\eta)\cos^2(\pi X'/2)}-1\right]\left[\cos(k\pi X')-\frac{1}{2}\delta_{k,0}\right], \quad (18)$$

$$r^{b,1}_{n,k}=\frac{\pi}{2}\int_{-1}^{1}dX\cos(n\pi X)\int_{-1}^{1}dX'R_g^{(0)}(|\tan(\frac{\pi}{2}X)-\tan(\frac{\pi}{2}X')|,|k_xd|)$$
$$\times f_0(X')\left[\frac{1+\eta}{1+\eta(2+\eta)\cos^2(\pi X'/2)}-1\right]\sin(k\pi X'), \quad (19)$$

$$r^{a,2}_{m,k}=\frac{\pi}{2}\int_{-1}^{1}dX\sin(m\pi X)\int_{-1}^{1}dX'R_g^{(0)}(|\tan(\frac{\pi}{2}X)-\tan(\frac{\pi}{2}X')|,|k_xd|)$$
$$\times f_0(X')\left[\frac{1+\eta}{1+\eta(2+\eta)\cos^2(\pi X'/2)}-1\right]\left[\cos(k\pi X')-\frac{1}{2}\delta_{k,0}\right], \quad (20)$$

$$r^{b,2}_{m,k}=\frac{\pi}{2}\int_{-1}^{1}dX\sin(m\pi X)\int_{-1}^{1}dX'R_g^{(0)}(|\tan(\frac{\pi}{2}X)-\tan(\frac{\pi}{2}X')|,|k_xd|)$$
$$\times f_0(X')\left[\frac{1+\eta}{1+\eta(2+\eta)\cos^2(\pi X'/2)}-1\right]\sin(k\pi X'). \quad (21)$$

Using Eqs. (17), in Fig. 6 for $\eta=1$ we plot dimensionless phase velocities for four most fast MEMPs with negative chirality and four most fast MEMPs with positive chirality as function of $2M_0/B_{ext}$. Here the values of W for $2M_0/B_{ext}\to 0$ coincide with the results obtained from Eqs. (9), (12).

To conclude, it has been shown that lateral inhomogeneous magnetic field allows the existence of the "magnetic gradient" or special magnetic-edge magnetoplasmons due to complex lateral structure of magnetic field distribution. We have obtained the eigen value problem that corresponds to the motion of charge density wave perpendicular to magnetic gradient. At low wave vector k_x magnetoplasmons have acoustic type dispersion, $\omega\propto k_x$. For non-monotonic distribution of magnetic field "magnetic gradient" magnetoplasmon may move in both directions. To solve eigen value problem we have used two types of numerical approaches: first is the grid method that diagonalizes large Hermitian matrix and second is semi-analytical approach that expand each eigen mode on the set of orthogonal functions. The latter approach needs less computing time and provides better accuracy for fastest positive and negative modes. However, the grid method is more universal and gives reasonable accuracy for larger amounts of fastest modes.

Acknowledgments
We are grateful to Lloyd W. Engel for many useful discussions on a possibility of MEMP, due to inhomogeneity of magnetic field, relevant experiments and experimental conditions. The research leading to these results has received funding from the European Union Seventh Framework Programme (FP7/2007-2013) under grant agreement nº PCOFUND-GA-2009-246542 and from the Foundation for Science and Technology of Portugal. We also acknowledge support by Brazilian FAPEAM grants: Universal Amazonas (Edital 021/2011) and PVS.

References

[1] Volkov V A and Mikhailov S A 1991 *Electrodynamics of Two-Dimensional Electron Systems in High Magnetic Fields*, in *Landau Level Spectroscopy, Modern Problems in Condensed Matter Sciences*, Ed. by G. Landwehr and E. I. Rashba (North-Holland, Amsterdam) vol 27.2 chapter 15 pp 855-907; Volkov V A and Mikhailov S A 1988 *Zh. Eksp. Teor. Fiz.* **94** 217 [1988 *Sov. Phys. JETP* **67** 1639]
[2] Kushwaha M S 2001 *Surface Science Reports* **41** pp 1-416
[3] Balev O G and Vasilopoulos P 1998 Phys. Rev. Lett. **81** 1481
[4] Khannanov M N, Fortunatov A A and Kukushkin I V 2009 *Pis'ma Zh. Eksp. Teor. Fiz.* **90** 740 [2009 *JETP Lett.* **90** 667
[5] Silva S and Balev O G 2010 *J. Appl. Phys.* **107** 104310
[6] Balev O G and Larkin I A 2013 *J. Phys.: Conf. Ser.* **456** 012023
[7] Larkin I A and Sukhorukov E V, Phys. Rev. **49**, 5498 (1994).
[8] Jackson J D 1999 *Classical Electrodynamics* 3d ed. (John Wiley&Sons, New York)